A Two-Base Mechanism for *Escherichia coli* ADP-L-*glycero*-D-*manno*-Heptose 6-Epimerase†

James P. Morrison and Martin E. Tanner*

Department of Chemistry, University of British Columbia, Vancouver, British Columbia, Canada V6T 1Z1

Received December 22, 2006; Revised Manuscript Received January 31, 2007

ABSTRACT: ADP-L-*glycero*-D-*manno*-heptose 6-epimerase (HldD or AGME, formerly RfaD) catalyzes the inversion of configuration at C-6″ of the heptose moiety of ADP-D-*glycero*-D-*manno*-heptose and ADP-L-*glycero*-D-*manno*-heptose. The epimerase HldD operates in the biosynthetic pathway of L-*glycero*-D-*manno*-heptose, which is a conserved sugar in the core region of lipopolysaccharide (LPS) of Gram-negative bacteria. Previous studies support a mechanism in which HldD uses its tightly bound $NADP^+$ cofactor to oxidize directly at C-6″, generating a ketone intermediate. A reduction of the ketone from the opposite face then occurs, generating the epimeric product. How the epimerase is able access both faces of the ketone intermediate with correct alignment of the three required components, NADPH, the ketone carbonyl, and a catalytic acid/base residue, is addressed here. It is proposed that the epimerase active site contains two catalytic pockets, each of which bears a catalytic acid/base residue that facilitates reduction of the C-6″ ketone but leads to a distinct epimeric product. The ketone carbonyl may access either pocket via rotation about the C-5″−C-6″ bond of the sugar nucleotide and in doing so presents opposing faces to the bound cofactor. Evidence in support of the two-base mechanism is found in studies of two single mutants of the *Escherichia coli* K-12 epimerase, Y140F and K178M, both of which have severely compromised epimerase activities that are more than 3 orders of magnitude lower than that of the wild type. The catalytic competency of these two mutants in promoting redox chemistry is demonstrated with an alternate catalytic activity that requires only one catalytic base: dismutation of a C-6″ aldehyde substrate analogue (ADP-β-D-*manno*-hexodialdose) to an acid and an alcohol (ADP-β-D-mannuronic acid and ADP-β-D-mannose). This study identifies the two catalytic bases as tyrosine 140 and lysine 178. A one-step enzymatic conversion of mannose into ADP-β-mannose is also described and used to make C-6″-substituted derivatives of this sugar nucleotide.

Lipopolysaccharide (LPS)[1] is the major component of the outermost surface of Gram-negative bacteria, and while a wealth of understanding of this glycolipid has been realized, its complexity and importance to biology ensure that LPS remains the focus of considerable research effort. LPS is comprised of three parts: lipid A (endotoxin), a core domain, and the immunogenic O-antigen repeat polymer (*1*, *2*). The core domain is a nonrepeating oligosaccharide consisting of 6−10 core sugars (*Escherichia coli* K-12) and contains the unusual higher-order sugars 3-deoxy-D-*manno*-oct-2-ulosonic acid (Kdo) and L-*glycero*-D-*manno*-heptose (L,D-Hep). Functionally, the core region is a barrier to antibiotics, as evidenced by studies of mutant strains of *E. coli* K-12 and other Gram-negative mutant bacteria that bear truncated LPS lacking core oligosaccharides (*3*, *4*). These mutant bacteria are viable but exhibit an increased susceptibility to hydrophobic antibiotics and reduced pathogenicity. Thus, the enzymes involved in the biosynthesis of higher-order sugars in the core region of LPS are potential therapeutic targets for the development of agents that could be used in tandem with available antibiotics.

L,D-Hep is derived from sedoheptulose 7-phosphate in the biosynthetic pathway summarized in Figure 1 (*5*, *6*). In the first step, the ketose is isomerized to the *manno*-aldose by the action of GmhA. D,D-Hep 7-phosphate is then subjected to the kinase activity of the bifunctional enzyme HldE to generate β-D,D-Hep 1,7-bisphosphate. This serves as the substrate of phosphatase GmhB, which cleaves the C-7 phosphate to give β-D,D-Hep 1-phosphate. The necessity of two enzymes and 1 equiv of ATP in the conversion of D,D-Hep 7-phosphate to β-D,D-Hep 1-phosphate differs from typical sugar nucleotide biosynthetic pathways, where a phosphomutase accomplishes a similar reaction without utilizing 1 equiv of ATP. Another notable difference in the heptose pathway of LPS biosynthesis is that a β-linked sugar nucleotide is generated. The second activity of HldE, the aldenylyltransferase activity, then converts β-D,D-Hep 1-phosphate to ADP-D,D-Hep. ADP-L,D-Hep is generated by a reversible epimerization catalyzed by the enzyme ADP-β-L-*glycero*-D-*manno*-heptose 6-epimerase (HldD or AGME, formerly RfaD), and finally, heptosyltransferases introduce L,D-Hep to the growing LPS structure.

† This research was supported by the Canadian Institutes of Health Research (CIHR).

* To whom correspondence should be addressed. Phone: (604) 822-9453. Fax: (604) 822-2847. E-mail: mtanner@chem.ubc.ca.

[1] Abbreviations: LPS, lipopolysaccharide; Kdo, 3-deoxy-D-*manno*-oct-2-ulosonic acid; L,D-Hep, L-*glycero*-D-*manno*-heptose; SDR, short-chain dehydrogenase/reductase; IPTG, isopropyl β-D-galactopyranoside; TBAHS, tetrabutylammonium bisulfate.

10.1021/bi602641m CCC: $37.00
Published on Web 02/23/2007

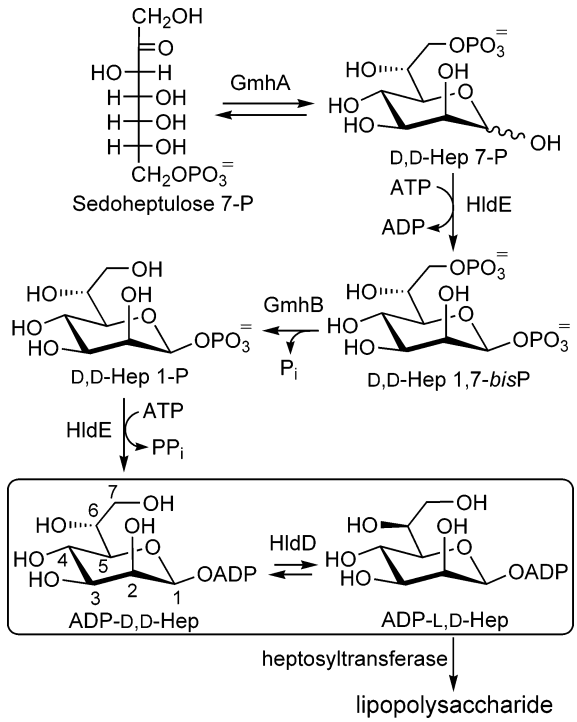

FIGURE 1: Biosynthesis of the LPS inner core sugar ADP-L,D-Hep. The reaction catalyzed by ADP-*β*-L-*glycero*-D-*manno*-heptose 6-epimerase (HldD) is boxed.

The mechanism of HldD is of interest as the chemistry occurs at an "unactivated" stereocenter lacking an acidic C−H bond (pK_a > 30) (*7*, *8*). This precludes the common epimerization strategy of deprotonation and reprotonation at the site of inversion. However, the epimerase tightly binds one nonexchangeable equivalent of NADP(H) and belongs to the short-chain dehydrogenase/reductase (SDR) superfamily of enzymes (*9*−*11*), indicating that a mechanism involving transient oxidation of the substrate is employed. Indeed, the structure of HldD complexed with ADP-α-glucose is known and clearly supports this notion as the sugar is bound in the intimate proximity of the nicotinamide ring of the cofactor (*10*). It is difficult to deduce the site of oxidation from this structure; however, as the electron density for the glucose is disordered in seven of the ten active sites in the unit cell, and two different bound conformations are observed in the three remaining active sites. This is likely due to the differing stereochemistry between ADP-α-D-glucose and ADP-*β*-L,D-Hep at both C-1″ and C-2″. Reasonable chemical mechanisms that involve transient oxidation at C-4″, C-6″, or C-7″ can be envisioned, and the distinction between them has been addressed (*12*−*14*). The observation that solvent-derived ^{18}O and ^{2}H isotopes are not incorporated into the product during catalysis does not support mechanisms that rely on proton transfer, or dehydration and rehydration, to invert the stereochemistry (*12*). The observation that ADP-*β*-L-*glycero*-D-*manno*-[6″-^{2}H]heptose retains its isotopic label at C-6″ during epimerization strongly supports a mechanism in which the C-6″ hydride (or deuteride) is transferred via $NADP^+$ to opposite faces of a ketone intermediate (*13*). In addition, it was observed that C-4″ and C-7″ deoxy substrate analogues also undergo epimerization, refuting mechanisms that rely on transient oxidation at these positions during catalysis (*12*). Further evidence that supports the direct C-6″ redox mechanism is

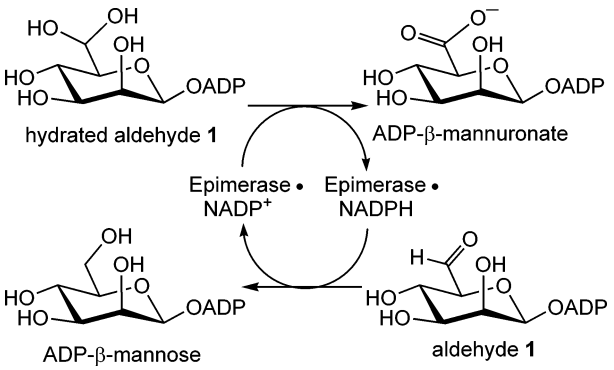

FIGURE 2: Substrate analogue ADP-*β*-D-*manno*-hexodialdose **1** dismutated to equal amounts ADP-*β*-D-mannose and ADP-*β*-D-mannuronate by catalytic amounts of HldD.

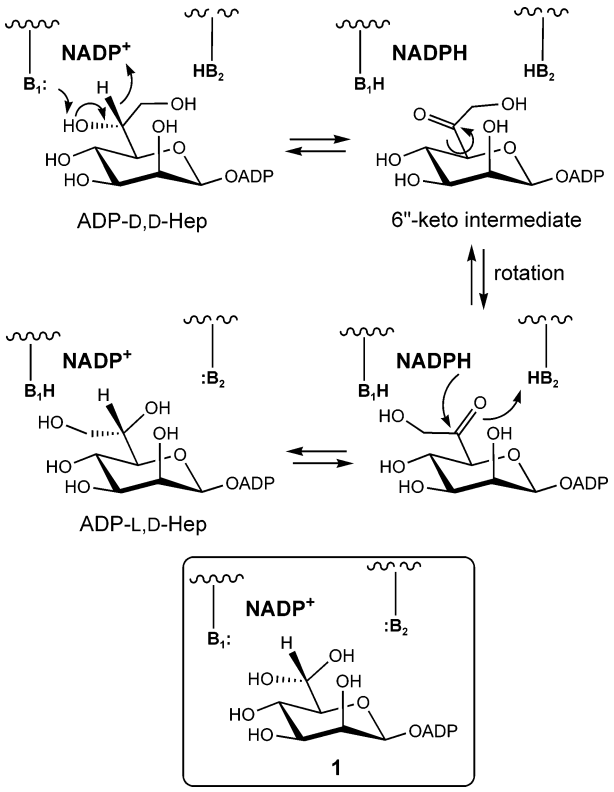

FIGURE 3: Proposed two-base mechanism for the reaction catalyzed by ADP-L,D-Hep 6-epimerase. B_1 and B_2 are active site acid/base residues. The inset shows the hydrated form of ADP-*β*-D-*manno*-hexodialdose **1** bound in the active site.

that a C-6″ aldehyde analogue of the ketone intermediate, ADP-*β*-D-*manno*-hexodialdose **1**, is observed to dismutate to alcohol and acid products in an overall redox-balanced fashion upon incubation with catalytic amounts of the epimerase (Figure 2) (*14*). The hydrated form of the aldehyde initially binds to the $NADP^+$ form of the enzyme and is oxidized to give the acid and the NADPH form of the enzyme. This form then binds the unhydrated aldehyde and reduces it to give the alcohol. Dismutase activity clearly demonstrates the ability of the epimerase to both oxidize and reduce sugar nucleotides at C-6″. The mechanism consistent with all observations involves the epimerase transiently oxidizing the natural substrate at C-6″ to generate a 6″-keto intermediate (Figure 3). A reorientation of the ketone and/or cofactor such that the opposite face of the carbonyl is exposed to the cofactor then takes place, and a subsequent reduction generates the epimeric product. To explain how

this non-stereospecific hydride transfer may occur, it is reasonable to assume that the ADP moiety and the tightly bound NADP(H) cofactor make many strong contacts within the active site and therefore do not undergo any major reorientations during catalysis. If this is the case, the epimerase must somehow allow binding of each of the epimeric substrates such that their C-6″ hydrogen is oriented toward the cofactor. We propose that there must be two pockets, each of which is capable of accommodating either the hydroxy or the hydroxymethylene substituent at C-6″. Each pocket contains an acid/base residue that is capable of deprotonating the C-6″ hydroxyl of a given epimer in the oxidation step of the reaction (B_1 for ADP-D,D-Hep in Figure 3). In this scenario, the ketone carbonyl simply flips into the opposite pocket via rotation about the C-5″−C-6″ bond and the other catalytic residue (B_2 in Figure 3) protonates the carbonyl during the reduction on the opposite face. Thus, the sites each effectively act as stereospecific dehydrogenases, but with opposing stereospecificity.

To probe this hypothesis, we sought to identify the putative catalytic bases using site-directed mutagenesis. Mutation of either base should result in a dramatic loss of epimerase activity since both sites must be active for an inversion of configuration to occur. Mutation of only one of these bases should not, however, abolish dismutase activity since only one functional site is required in this process. If one considers the oxidation of the hydrated aldehyde, it is apparent that both sites will contain a hydroxyl group (inset in Figure 3), and either base should be sufficient for this step of the dismutation process. Similarly, during the reduction step of dismutation, the aldehydic carbonyl could occupy either site and hydride transfer could still occur. Thus, the dismutation reaction serves as an important control reaction since it tests for mutants still capable of catalyzing only one of the two stereoselective hydride transfers. The key catalytic acid/base residues can therefore be identified by finding mutants that exhibit dramatically reduced epimerase activity yet retain significant dismutase activity.

In this work, we describe evidence that supports a two-base mechanism in which Tyr140 and Lys178 are the key catalytic acid/base residues. A one-step enzymatic conversion of mannose into ADP-*β*-mannose is also described and used to make C-6″-substituted derivatives of this sugar nucleotide.

EXPERIMENTAL PROCEDURES

Chemicals were purchased from Sigma-Aldrich and used without further purification unless otherwise noted. Dry methylene chloride and pyridine were distilled fresh using CaH_2 as a drying agent. Recombinant hexahistidine-tagged enzymes HldD and HldE (genes cloned previously from *E. coli* K-12 W3110) were prepared with the aid of the pET-30 Xa/LIC vector (Novagen) as previously described (*12*, *14*). Inorganic pyrophosphatase (from yeast) was purchased from Roche Diagnostics (Indianapolis, IN). ^{1}H NMR spectra were obtained on Bruker AV 300 and AV400 instruments at a field strength of 300 or 400 MHz. Proton-decoupled ^{31}P NMR spectra were obtained at 121.5 or 162 MHz. Mass spectrometry was performed by electrospray ionization (ESI-MS) using an Esquire LC mass spectrometer. HPLC was performed using a Waters 600 instrument with a Waters 2996 photodiode array detector. The substrate ADP-D,D-Hep was prepared as described previously (*12*, *13*).

*Synthesis of 1,2,3,4-Tetra-O-trimethylsilyl-α-D-manno-hexodialdose **2***. Aldehyde **2** was prepared by oxidation of known compound 1,2,3,4,6-penta-*O*-(trimethylsilyl)-α-D-mannopyranose (*15*), using a method developed for the *gluco* epimer (*16*). The pentasilylation of mannose was as follows. To a solution of 1.00 g of mannose (5.60 mmol) in 5.5 mL of dry pyridine was added 4.25 mL of chlorotrimethylsilane (33.6 mmol, 6.0 equiv) at room temperature. After the mixture had been stirred for 6 h, 40 mL of diethyl ether was added to the mixture and the organic layer was washed twice with 2 × 30 mL of water and once with 30 mL of brine. The organic layer was then dried over magnesium sulfate, and the solvent was evaporated in vacuo to yield 2.3 g of clear, light yellow oil. A ^{1}H NMR spectrum of the crude product revealed an ∼3:1 α/*β* anomeric mixture. The anomeric mixture was purified by silica gel column chromatography with a 3:1 petroleum ether/CH_2Cl_2 mixture to give 2.05 g of 1,2,3,4,6-penta-*O*-(trimethylsilyl)-D-mannopyranose as a colorless oil (3.79 mmol, 68% yield, R_f = 0.3, MS *m*/*z* 563.2 $[M + Na]^+$). Earlier column fractions contained one anomer, determined to be the α-anomer by comparison with literature ^{1}H NMR data (*15*). For ease of product identification, the α-anomer was carried on exclusively in the next synthetic steps. Chromium trioxide (1.72 g, 17.2 mmol), 60 mL of dry CH_2Cl_2, and 2.8 mL of dry pyridine were stirred at room temperature for 30 min and then chilled on ice for 5 min. A solution of 1.55 g of 1,2,3,4,6-penta-*O*-(trimethylsilyl)-α-D-mannopyranose (2.86 mmol) in 4 mL of dry CH_2Cl_2 was added dropwise, and the reaction mixture was allowed to stir at 0 °C. After 1 h, the dark brown reaction mixture was filtered through silica gel, which was then rinsed with 2 × 60 mL of ethyl acetate. The filtered crude material was dried in vacuo to give 1.6 g of clear yellow oil. Purification by column chromatography (1:1 CH_2Cl_2/petroleum ether mixture to 100% CH_2Cl_2) gave 243 mg of **2** as a colorless oil (0.52 mmol, 18% yield, R_f = 0.1−0.4 streak in CH_2Cl_2): ^{1}H NMR ($CDCl_3$) *δ* 9.67 (s, 1H, H6), 5.09 (s, 1H, H1), 4.06 (d, 1H, $J_{4,5}$ = 5.4 Hz, H5), 4.03 (dd, 1H, $J_{3,4}$ = 5.6 Hz, $J_{4,5}$ = 5.6 Hz, H4), 3.81 (d, 1H, $J_{3,4}$ = 4.3 Hz, H3), 3.67 (dd, 1H, $J_{3,4}$ = 4.8 Hz, $J_{2,3}$ = 2.2 Hz, H2), 0.16, 0.11, 0.11, 0.10 [4 × s, 36H, $(CH_3)_3Si$]; ESI-MS *m*/*z* 521.1 $[M + MeOH + Na]^+$ (hemiacetal with methanol solvent).

*Synthesis of Adenosine Diphosphate-β-D-manno-Hexodialdose **1***. Deprotection of aldehyde **2** to give D-*manno*-hexodialdo-1,5-pyranose was carried out using a method adapted from the literature preparation of the *gluco* epimer (*16*). Aldehyde **2** (119 mg, 0.255 mmol) was stirred in 1.5 mL of a 1 mg/mL K_2CO_3 solution in methanol at room temperature for 1 h. The deprotected mannose dialdehyde could be isolated by precipitation of the product by cooling to −20 °C and addition of a 1:1 diethyl ether/ethyl acetate mixture. ^{1}H NMR (D_2O) of the isolated white solid revealed a complex mixture of signals, consistent with compounds of this type (*16*, *17*): ESI-MS *m*/*z* 379.0 $[2M + Na]^+$. In a more streamlined synthetic approach, D-*manno*-hexodialdo-1,5-pyranose was not isolated, but the crude mixture was carried forward as follows. The crude solution was diluted to 10 mL to create a solution containing 0.54 mmol of ATP (2.1 equiv), 150 mM triethanolamine (pH 7.5), 2 mM $MgCl_2$, 2.6 mg of HldE, 25 *μ*g of inorganic pyrophosphatase (from yeast, Roche), and 10% D_2O. The reaction mixture was

incubated at 25 °C, and progress was monitored by ^{31}P NMR spectroscopy. After 24 h, the product signals at −10 and −12 ppm stopped increasing in intensity, so the solution was filtered by centrifugal filtration (Amicon Ultra-4, 10 000 MWCO), loaded onto an anion exchange column (DE-52 resin) equipped with a UV detector (λ_{obs} = 254 nm), and eluted with a gradient of 0.1 to 0.5 M triethylammonium bicarbonate buffer (pH 7.5). Product-containing fractions were lyophilized and pooled. The already known product was identified by ^{1}H and ^{31}P NMR spectroscopy and mass spectroscopy (*14*). Quantification of the product by A_{259} measurements in aqueous solution [100 mM potassium phosphate (pH 7.0); ϵ = 15 400 M^{-1} cm^{-1}] found 0.178 mmol of **1** was isolated (70% yield from **2**). The purity was estimated to be 95% by HPLC.

Site-Directed Mutagenesis and Preparation of HldD Mutants. Plasmids bearing the mutated HldD genes were prepared using the QuikChange site-directed mutagenesis kit from Stratagene. Oligonucleotide primers used are listed below, with the mutated nucleotides underlined. Primers for the Y140F mutant were as follows: 5′-GAAAAACCGTTGAACGTCTTCGGTTACTCAAAATTCCTG-3′ (forward) and 5′-CAGGAATTTTGAGTAACCGAAGACGTTCAACGGTTTTTC-3′ (reverse). Primers for the K178M mutant were as follows: 5′-GTGAAGGCCATATGGGCAGCATGGCGAG-3′ (forward) and 5′-CTCGCCATGCTGCCCATATGGCCTTCAC-3′ (reverse). Primers for the K208M mutant were as follows: 5′-GAAGGTAGCGAGAACTTCATGCGCGACTTCGTCTATGTG-3′ (forward) and 5′-CACATAGACGAAGTCGCGCATGAAGTTCTCGCTACCTTC-3′ (reverse). Primers for the D210N mutant were as follows: 5′-GAACTTCAAACGCGATTTCGTCTATGTGGGCG-3′ (forward) and 5′-CGCCCACATAGACGAAATCGCGTTTGAAGTTC-3′ (reverse). Double mutant Y140F/K178M was prepared by mutagenesis PCR of the Y140F plasmid with K178M primers. Mutated gene sequences were confirmed by sequencing the entire gene. Overexpression of the plasmids encoding Y140F, K178M, D210M, and D210N mutants and wild-type hexahistidine-tagged HldD (at 37 °C) and purification of the resulting protein (at 23 °C) were identical as reported previously for wild-type hexahistidine-tagged HldD (*14*). The K178M and Y140F/K178M mutants were generated by overexpressing the corresponding plasmids and purifying the resulting protein with the same protocol, only at lower temperatures. In the preparation of the K178M mutant, cells were grown to midlog phase at 37 °C, then induced with isopropyl β-D-galactopyranoside (IPTG), and grown at 23 °C to an OD_{600} of ∼1.6. In the preparation of the Y140F/K178M double mutant, cells were grown at 23 °C to midlog phase, then induced with IPTG, and grown at 18 °C to an OD_{600} of ∼1.6. Both K178M and Y140F/K178M were purified by nickel affinity chromatography at 4 °C. All enzyme varients were dialyzed, flash-frozen, and stored at −80 °C at ∼25−50 μM as described previously (*12*, *14*). When desired, an aliquot of HldD was thawed at room temperature and $NADP^+$ was added to give a cofactor concentration of 200 μM. The epimerases were incubated with $NADP^+$ for 30 min at room temperature, and then buffer was exchanged with 10 mM potassium phosphate (pH 7.0) (deuterated buffer for NMR experiments) by centrifugal filtering (Amicon Ultra-4, 10 000 MWCO) at 6000*g* to affect a 1000-fold dilution of the cofactor. Protein concentrations were measured using Bradford dye.

Measurement of Epimerase Activity by NMR Spectroscopy. In a parallel incubation in NMR tubes, the appropriate version of HldD was added to a D_2O solution containing ADP-D,D-Hep and 10 mM potassium phosphate buffer (pH 7.0). The tube was inverted three times to allow mixing of the 580 μL solution containing 2.7 mM substrate and 2.65 μM enzyme. Conversion of ADP-D,D-Hep to ADP-L,D-Hep was followed using both ^{1}H and ^{31}P NMR spectroscopy at 23 °C.

Measurement of Dismutase Activity by HPLC. In five 800 μL snap-top tubes, aldehyde **1** in 10 mM potassium phosphate buffer (pH 7.0) was equilibrated at 37 °C for 5 min (total volume of 500 μL). The parallel incubations were initiated by adding the appropriate version of HldD to each tube (either wild type, Y140F, K178M, Y140F/K178M, or a control which contained no enzyme), inverting the tubes three times, and returning the tubes to the incubation bath. Substrate and enzyme concentrations of the 500 μL solutions were 1 mM and 0.5 μM, respectively. At appropriate intervals (15 min for the wild type and 30 or 60 min for the mutants), 50 μL aliquots were removed and flash-frozen in liquid nitrogen. Immediately prior to injection, the aliquots were thawed by addition of 50 μL of room-temperature deionized water, and the solution was injected within 10 s of thawing. The reversed-phase ion-pair HPLC protocol using a Waters Spherisorb ODS II 5 μm (250 mm × 4.6 mm) column was adapted from the literature (*18*). Two mobile phases were used: mobile phase A containing 50 mM potassium phosphate (pH 7.0) and 2.5 mM tetrabutylammonium bisulfate (TBAHS) and mobile phase B containing 50 mM potassium phosphate (pH 7.0), 2.5 mM TBAHS bisulfate, and 50% acetonitrile. A linear gradient from 2.5 to 30% mobile phase B over 30 min at a flow rate of 1 mL/min eluted the ADP sugars, which were detected at 259 nm. Aldehyde **1** and ADP-mannose coeluted at 19 min, and ADP-mannuronate eluted at 23 min.

RESULTS

One-Step Synthesis of ADP-β-Mannose and a C-6″-Azido Derivative. The biosynthetic strategy that *E. coli* uses to synthesize β-D,D-Hep 1-phosphate from D,D-Hep 7-phosphate involves the kinase activity of HldE and the phosphatase GmhB (Figure 1). This strategy is somewhat unusual, since what is effectively a net transfer of a phosphate from C-7 to C-1 requires two enzymes. Classically, in sugar nucleotide biosynthesis, similar transformations are accomplished by a single enzyme (a mutase) without using a full equivalent of ATP (for example, phosphoglucomutase). The ATP-dependent biosynthetic strategy prompted us to analyze whether alternate substrates could be phosphorylated by the kinase activity of HldE. We thought that by incubating mannose and high concentrations of phosphate buffer with HldE, both mannose and phosphate could bind in the HldE active site simultaneously, mimicking the natural substrate, D,D-Hep 7-phosphate (Figure 4). Phosphorylation of the "broken" substrate would generate β-mannose 1-phosphate. We have previously demonstrated that β-mannose 1-phosphate is a substrate for the phosphorylase activity of HldE (*14*), so we anticipated that mannose would be converted to ADP-β-

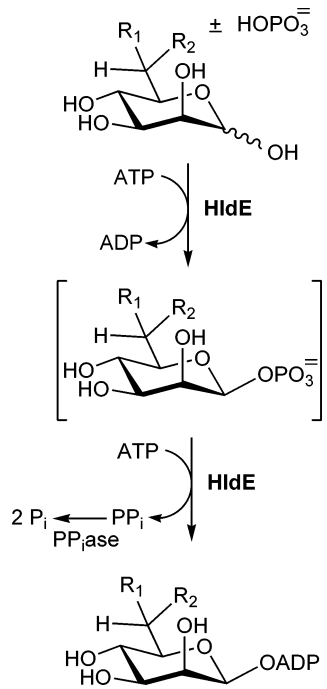

FIGURE 4: Both kinase and pyrophophorylase activities of HldE are exploited in generating ADP-β-D-mannose (R_1 = OH, and R_2 = H), ADP-β-D-*manno*-hexodialdose **1** (hydrated form; R_1 = OH, and R_2 = OH), and ADP-6″-azido-6″-deoxy-β-D-mannose (R_1 = N_3, and R_2 = H).

mannose, without any requirement for the phosphatase GmhB. When mannose, ATP, and HldE were incubated in the presence of varying concentrations of phosphate (up to 400 mM), signals that can be attributed to ADP-β-mannose were observed by ^{31}P NMR spectroscopy. The ADP-β-mannose produced was purified and structurally characterized by comparison with an authentic sample, which had been synthesized previously in six steps (*14*). Somewhat surprisingly, product also formed in the control containing no phosphate buffer (buffered with triethanolamine instead). Furthermore, the rate of product formation was actually higher in the control reaction. Evidently, the kinase activity of HldE does not require a phosphate bound in its active site, nor does the presence of phosphate accelerate the phosphorylation. Consequently, all the subsequent incubations with HldE were carried out in triethanolamine buffer with no added phosphate, as this fortuitous discovery simplifies the purification of the ADP-sugar product by anion exchange chromatography.

We further probed the substrate specificity of HldE to determine if stereoisomers of mannose would be tolerated (Figure 4). The D-aldoses glucose, altrose, and talose all differ from mannose in the stereochemistry at C-2, C-3, and C-4, respectively. Incubation of these sugars with HldE for 3 days at 37 °C did not generate ADP-sugar or ADP as determined by ^{31}P NMR spectroscopy; however, addition of mannose on the third day generated ADP-mannose in high yield after only 5 h.

As the β-linked ADP-mannosyl configuration is notoriously susceptible to intramolecular attack of the C-2″ hydroxyl on the β-phosphate, generating mannose 1,2-cyclic phosphate and AMP (*19*), we sought to make a stable C-2″-derivatized version of the substrate using HldE. Unfortunately, neither 2-deoxymannose, 2-deoxy-2-fluoromannose,

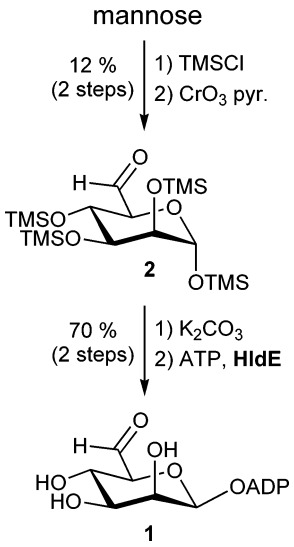

FIGURE 5: Synthesis of ADP-β-D-*manno*-hexodialdose **1** in four steps from mannose. In aqueous solution, **1** occurs predominantly as a hydrated aldehyde.

2-amino-2-deoxymannose, nor *N*-acetylmannosamine proved to be a substrate, as determined by the 3 day incubation test outlined above.

To probe the tolerance of HldE to functionality at C-6, 6-azido-6-deoxymannose appeared to be the most accessible C-6-derivatized version of mannose available. The azide was prepared in two steps via a known preparation (*20*), and upon incubation with HldE, two doublets characteristic of sugar nucleotides appeared in the ^{31}P NMR spectrum. Purification of the product and further characterization, including ^{1}H NMR spectroscopy and mass spectral analysis, confirm that ADP-6″-azido-6″-deoxy-β-D-mannose was in fact formed (Supporting Information). Encouraged by this result, we designed a concise chemoenzymatic synthesis of ADP-β-D-*manno*-hexodialdose **1**.

*Chemoenzymatic Synthesis of Adenosine Diphosphate-β-D-manno-hexodialdose **1***. Aldehyde **1**, which contains the aforementioned problematic β-mannosyl diphosphate linkage, is further complicated by the presence of an aldehyde functionality at C-6″. These two complicating factors make conventional chemical synthesis of **1** challenging but also render **1** unstable such that decomposition occurs in solution, even at neutral pH during extended incubation. This is reflected by the fact that the previous synthesis yielded **1** with a compromised purity of ~70% (*14*). To facilitate studies requiring compound **1**, an abbreviated synthesis using mild conditions and yielding **1** with enhanced purity is extremely attractive from a practical viewpoint. Thus, we designed a new synthesis taking advantage of the newly discovered substrate flexibility of HldE (Figure 5). The chemical portion of the chemoenzymatic synthesis of **1** is based upon a synthesis of glucose 1,6-dialdehyde (*16*). Persilylation of mannose, followed by selective oxidation of the primary silyl ether, gives the protected dialdehyde, **2**, which is stable to silica gel chromatography and storage for a few days at −20 °C. Deprotection of **2** under mildly basic conditions gave mannose 1,6-dialdehyde, which could be isolated by precipitation. Even though the aldehydes of mannose 1,6-dialdehyde are homotopic, the compound exhibits a complex ^{1}H NMR spectrum, consistent with the notion that it exists as a mixture of species in solution. This

likely includes a $^1C_4$ chair with a second hemiacetal formed between the axial C-3 hydroxyl and the C-6 aldehyde, which has been observed for galactose 1,6-dialdehyde (*17*). Incubation of mannose 1,6-dialdehyde with catalytic amounts of HldE and 2.1 equiv of ATP resulted in the generation of **1**, consistent with the observation that HldE is tolerant to functionality at C-6. Most attractively, the purity of **1** generated in this abbreviated synthesis (95%, as determined by HPLC) is superior to that generated by the previous synthesis.

Site-Directed Mutagenesis and Overexpression of Mutants. Candidates for the acid/base residues were identified using the available crystal structure of HldD with ADP-α-D-glucose bound (*10*). ADP-α-D-glucose differs significantly from the natural substrate in the stereochemistry at C-1″ and C-2″ and also lacks the C-6″ hydroxymethylene group. Perhaps not surprisingly, the sugar moiety was not well-resolved in the crystal structure and was only modeled in three of the ten active sites of the unit cell. Further, the glucose moiety occurs in two significantly different orientations in these three cases. Consequently, this structure bears only a limited relationship to that of the true Michaelis complex. Nevertheless, the $NADP^+$ cofactor is in the proximity of the glucose moiety, as is the conserved residue tyrosine 140. Both sequence and structural comparison between HldD and other well-studied SDR enzymes indicate that tyrosine 140 along with serine 116 and lysine 144 form the conserved catalytic triad that is a signature of this family (*10*). Within this triad, tyrosine likely serves as the key acid/base catalyst and thus was targeted for mutagenesis. In addition to tyrosine 140 of the catalytic triad, all other potential acid/base residues positioned within 10 Å of the C-4 position of $NADP^+$ were sought out. Several other potentially basic residues were identified: lysine 178, lysine 208, and aspartate 210. In light of this, the following mutant epimerases were prepared: Y140F, K178M, K208M, and D210N. Following the initial evaluation of the single mutants, a Y140F/K178M double mutant was also prepared.

Plasmids encoding hexahistidine-tagged mutant and wild-type enzymes were overexpressed in *E. coli*, and the resulting proteins were purified by nickel affinity chromatography. The Y140F, K208M, and D210N mutants were obtained in good yield (≈20 mg/L) using the same conditions that were employed with the wild-type enzyme. With K178M and Y140K/K178M, however, both expression and purification had to be carried out at lower temperatures and lower yields were obtained (≈10 mg/L).

To probe for correct folding of the mutant enzymes, their ability to bind the NADP(H) cofactor was assessed using UV spectroscopy. Wild-type HldD is known to tightly bind 1 equiv of cofactor (*9*). The cofactor remains bound during purification of the enzyme and is released only upon denaturation. Thus, in previous studies of HldD, no exogenous $NADP^+$ was required for full enzymatic activity (*12*−*14*). Typically, purified recombinant HldD contains a mixture of $NADP^+$ and NADPH such that an absorption band at 355 nm due to the bound NADPH is observed. A ratio of protein absorbance to bound NADPH absorbance ($A_{278}/A_{350} = 19$) has been reported for non-His-tagged recombinant epimerase (*9*). The ability of the epimerase to bind cofactor implies proper folding; thus, we measured this readily observable property of the mutant epimerases. The wild type and Y140F, K208M, and D210N mutants were found to have identical UV profiles, indicating a normal ratio of NADPH bound to these proteins. In contrast, the UV spectra of the K178M and Y140F/K178M mutants conspicuously lacked a long wavelength band, indicating a lack of cofactor bound to these mutants. This was confirmed upon addition of sodium borohydride, which did not generate a 355 nm band in the spectra of these mutants. Conversely, the addition of sodium borohydride to the wild-type, Y140F, K208M, and D210N proteins noticeably enhanced the bound NADPH band. Evidently, K178M and Y140F/K178M had been isolated as apoenzymes. Apoenzymes may be more prone to in vivo denaturation and degradation, and this may explain why the yields of these mutants were lower. To reconstitute these mutants with a cofactor, they were incubated with 200 μM $NADP^+$ for 30 min at room temperature and then the excess cofactor was removed via centrifugal filtration (≈1000-fold dilution of unbound cofactor). Fortunately, a sodium borohydride reduction of the resulting samples gave UV spectral profiles that were similar in both wavelength and intensity to those of the reduced wild-type, Y140F, K208M, and D210M proteins. These observations indicate that while K178M and Y140F/K178M are isolated as apoenzymes, they may be reconstituted with $NADP^+$ and will bind the cofactor with sufficient affinity to be isolated as approximately 1:1 complexes. While binding of the cofactor implies that the mutants are properly folded, a more convincing assay involves measurement of catalytic activity, which is addressed in the next section.

Table 1: Epimerase and Dismutase Activities of Mutant Epimerases

	epimerase % activity[a]	dismutase % activity[a]
wild type	100	100
Y140F	0.08	20
K178M	0.1	5
K208M	85	nd[b]
D210N	90	nd[b]
Y140F/K178M	<0.01[c]	<0.2[c]

[a] Versus that of His-tagged wild-type HldD. [b] Not determined. [c] Product not observed. Estimated maximum possible activity based on an ability to detect 2% epimerized products and 0.1% oxidized products.

Epimerase and Dismutase Activities of Mutant HldD versus the Wild Type. Attempts to monitor the epimerization kinetics by HPLC were unsuccessful due to an inability to cleanly separate the epimers. Instead, the epimerization was monitored using ^1H NMR spectroscopy by observing the well-resolved H-5″ signals of the two epimers. While ^1H NMR integration is not known for its sensitivity, monitoring the first 15% of conversion gave a measure of activity that was sufficient to outline the dramatic effects incurred upon mutagenesis of the key active site residues. Thus, the epimerase activities of the mutants were measured in a NMR tube using a substrate concentration of 2.7 mM, far in excess of the wild-type K_m value (0.1 mM) (*9*). Under these conditions, the His-tagged wild-type epimerase exhibited a specific catalytic activity of 2.7 ± 0.8 μmol min^{-1} mg^{-1} at 23 °C. Table 1 shows the activities of the mutants normalized to that of the wild-type enzyme (100%). The K208M and D210N mutants displayed activity similar to that of the wild type; however, the Y140F and K178M mutants displayed epimerase activity at least 3 orders of magnitude lower than that of the wild type.

These observations suggested either that tyrosine 140 and lysine 178 are the two catalytic bases or that they play some other role that is essential for catalysis. It was plausible that catalytic activity was lost in these mutants due to improper folding or local disruption of the active site. To address this concern, the ability of these two mutants to catalyze dismutation was assessed. Since dismutation does not have a stereochemical requirement for two bases, only one base is sufficient for catalysis, and the ability of the mutant to promote a stereospecific hydride transfer may be assessed.

To monitor the dismutation, HPLC was used since the additional negative charge on ADP-mannuronate allows easy separation from **1** and ADP-mannose. Employing a fixed-time assay, we carried out incubations using 1 mM aldehyde **1**, and the first 5% of conversion was assessed. In this manner, His-tagged wild-type HldD was found to have a measured dismutase specific activity of 0.20 ± 0.04 μmol min^{-1} mg^{-1} at 37 °C. Increasing the concentration of **1** to 2 mM did not increase this activity, demonstrating that the substrate concentration is saturating. When Y140F and K178M were examined, they were found to retain reasonable levels of dismutase acitivity [20 and 5%, respectively (Table 1)]. Most importantly, the magnitude of the loss of dismutase activities of Y140F and K178M compared to that of the wild type is not nearly as severe as the loss of epimerase activity, consistent with the notion that dismutation requires only one catalytic residue. To confirm that dismutation does require one catalytic residue, dismutase activity of the Y140F/K178M double mutant was assessed. The double mutant did not exhibit significant dismutase activity, as anticipated, and thus, the dismutase activities observed for Y140F and K178M reflect the catalytic activity of mutants with one catalytic residue. The fact that Y140F and K178M are proficient dismutases but severely impaired epimerases indicates that tyrosine 140 and lysine 178 do not simply play structural roles. This provides evidence that they are the catalytic residues in a two-base model.

DISCUSSION

In this work, a single-step installation of a β-ADP group onto C-6-derivatized mannoses is described. This enables a rapid preparation of ADP-β-D-*manno*-hexodialdose **1** that is used in conjunction with mutagenesis studies to probe the active site of ADP-L-*glycero*-D-*manno*-heptose 6-epimerase. The observation that two mutants have severely compromised epimerase activity, and that these same mutants retain reasonable levels of dismutase activity, is fully consistent with the proposed two-base mechanism (Figure 3). In the forward direction, from ADP-D,D-Hep to ADP-L,D-Hep, the first base (B_1) functions to deprotonate the C-6″ hydroxyl which is simultaneous with hydride abstraction. A rotation around the C-5″−C-6″ bond of the resulting ketone intermediate presents the opposite face of the carbonyl to the reduced cofactor. In this conformation, the first acid/base residue is now inappropriately positioned to protonate the carbonyl, and thus, a second acid/base residue (B_2) has been recruited to fulfill this role. Reduction of the carbonyl by NADPH coordinated with protonation of the carbonyl oxygen generates the ADP-L,D-Hep epimer. In the opposite reaction direction, the two acid/base residues simply reverse their roles.

Since both sites are required for a non-stereospecific reduction of the ketone intermediate that leads to epimerization, mutation of either residue will severely cripple this process. The dismutase reaction, however, does not have such a stereochemical requirement, and therefore, the single mutants may still exhibit considerable dismutase activity. This is reminiscent of dehydrogenases such as horse liver alcohol dehydrogenase that exhibit dismutase activity yet are known to catalyze highly stereospecific hydride transfer reactions (*21*−*27*). In the Tyr140Phe and Lys178Met mutants of the epimerase, the dismutase activity was only moderately reduced (5- and 20-fold, respectively), indicating that either site was operational in a manner independent of the other. The observed reduction in dismutase activity was likely due to disruption of charge−charge or charge−dipole interactions and hydrogen bonding patterns that would be induced in the active site upon mutation and could affect the adjacent site to a certain extent during catalysis. The observation that a double mutant was essentially devoid of dismutase activity supports the notion that at least one of these residues is required for a hydride transfer event to occur.

The observation that Tyr140 serves as one of the catalytic bases in the epimerase reaction is not surprising given that HldD is a member of the SDR superfamily. SDR superfamily members contain a conserved catalytic triad consisting of Ser/Thr, Tyr, and Lys residues (*28*, *29*), which in HldD are Ser116, Tyr140, and Lys144, respectively (*10*). The roles of these conserved residues in the promotion of oxidation of the hydroxyl have been reviewed in SDR enzymes that operate on sugar nucleotides (*30*). In all cases, the tyrosine residue is thought to act as the catalytic base that removes the hydroxyl group proton during oxidation of an alcohol (or protonates the carbonyl during a reduction step). In most cases, the tyrosine is thought to deprotonate the substrate directly (*30*), but it may occur through a proton shuttle involving the triad serine in one case (*31*, *32*). With the XDP-hexose 4,6-dehydratases, transient oxidation is used to facilitate an overall dehydration process and hydride transfers to and from the same face of the hexose ring occur (*33*, *34*). In these cases, the catalytic triad provides all of the residues required for the hydride transfer steps. A similar scenario exists with enzymes such as dTDP-6-deoxy-L-*lyxo*-4-hexulose reductase (*35*), GDP-fucose synthetase (*36*, *37*), and GDP-mannose 3,5-epimerase (*38*), where hydride transfers occur only on one face of a carbonyl group. In the case of epimerases that utilize a direct hydride transfer mechanism, however, there is a requirement to deliver a hydride to both faces of a carbonyl intermediate. The best understood of these enzymes is UDP-galactose 4-epimerase, an SDR family member that shares considerable structural homology with HldD yet uses a "one-base" mechanism. This enzyme, along with the related UDP-*N*-acetylglucosamine 4-epimerases (*39*), initiates catalysis by hydride abstraction at C-4″ to give a 4-hexulose intermediate (Figure 6) (*31*, *32*, *40*). The hexulose portion of the bound intermediate then rotates within the active site to expose the opposite face of the carbonyl to the NADH cofactor (*40*, *41*). Reduction then generates the stereoisomeric product. This reaction is somewhat unique, however, in that the C-4 position lies on a pseudo-C-2 axis that links the hexose to the nucleotide. Thus, rotating the intermediate by 180° within the active site can be accomplished without any dramatic movement of the UDP

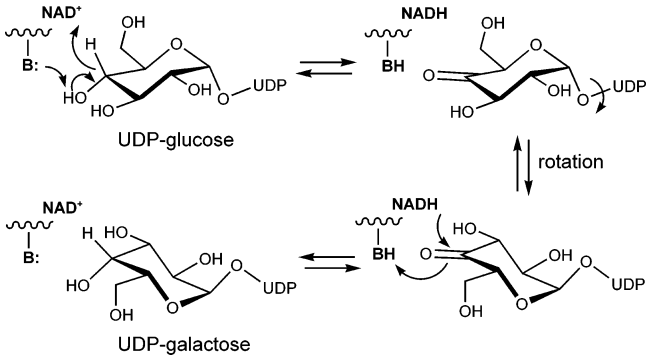

FIGURE 6: Established one-base mechanism of UDP-galactose 4-epimerase that involves the transient oxidation at C-4″ which generates a ketone intermediate. Rotation of the sugar moiety within the active site allows reduction from the opposite face of the ketone, generating the epimeric product (*40*, *41*).

moiety and can effectively place either face of the carbonyl in the same catalytic site. In this enzyme, it has been well-established that both of the hydride transfer steps are carried out by the same catalytic triad and the Tyr/Ser diad promotes each of the proton transfer events. A similar scenario has been put forward for the enzyme CDP-tyvelose 2-epimerase (*42*, *43*); however, the movement that exchanges the faces of the carbonyl is much more difficult to envision.

With ADP-heptose 6-epimerase, it seemed reasonable to expect that two bases would be required for catalysis, and the studies in this paper suggest it is supplied by Lys178. While a residue at this position is not normally involved in hydride transfer steps with other SDR family members, a recent study of GDP-mannose 3,5-epimerase suggests that a lysine in an analogous position serves to promote the deprotonation at C-3″ or C-5″ to form enolate intermediates (*38*). While the work described herein implicates Tyr140 and Lys178 as the acid/base residues required for catalysis, it does not distinguish which residue deprotonates the hydroxyl group of a given epimer. An inspection of the crystal structure suggests that Tyr140 deprotonates ADP-L,D-Hep and Lys178 deprotonates ADP-D,D-Hep; however, given the disordered nature of the bound sugar nucleotide, it is a speculative assignment. Further studies will be required to make this distinction.

ACKNOWLEDGMENT

We thank Dr. Jay A. Read and Dr. Raef A. Ahmed for the samples of (and synthetic precursors to) ADP-D,D-Hep used in this study.

SUPPORTING INFORMATION AVAILABLE

Descriptions of the enzymatic synthesis of ADP-β-D-mannose and the chemoenzymatic synthesis of ADP-6″-azido-6″-deoxy-β-D-mannose, in addition to a ^{1}H NMR spectrum of ADP-6″-azido-6″-deoxy-β-D-mannose. This material is available free of charge via the Internet at http://pubs.acs.org.

REFERENCES

1. Raetz, C. R. H., and Whitfield, C. (2002) Lipopolysaccharide endotoxins, *Annu. Rev. Biochem. 71*, 635−700.
2. Raetz, C. R. H. (1996) in *Escherichia coli and Salmonella* (Neidhardt, F. C., Ed.) pp 1035−1063, American Society for Microbiology, Washington, DC.
3. Coleman, W. G. J., and Leive, L. (1979) Two mutations which affect the barrier function of the *Escherichia coli* K-12 outer membrane, *J. Bacteriol. 139*, 899−910.
4. Vaara, M. (1993) Outer membrane permeability barrier to azithromycin, clarithromycin, and roxithromycin in Gram-negative enteric bacteria, *Antimicrob. Agents Chemother. 37*, 354−356.
5. Kneidinger, B., Marolda, C., Graninger, M., Zamyatina, A., McArthur, F., Kosma, P., Valvano, M. A., and Messner, P. (2002) Biosynthesis pathway of ADP-L-*glycero*-β-D-*manno*-heptose in *Escherichia coli*, *J. Bacteriol. 184*, 363−369.
6. Valvano, M. A., Messner, P., and Kosma, P. (2002) Novel pathways for biosynthesis of nucleotide-activated glycero-manno-heptose precursors of bacterial glycoproteins and cell surface polysaccharides, *Microbiology 148*, 1979−1989.
7. Samuel, J., and Tanner, M. E. (2002) Mechanistic aspects of enzymatic carbohydrate epimerization, *Nat. Prod. Rep. 19*, 261−277.
8. Tanner, M. E. (2002) Understanding nature's strategies for enzyme-catalyzed racemization and epimerization, *Acc. Chem. Res. 35*, 237−246.
9. Ding, L., Seto, B. L., Ahmed, S. A., and Coleman, W. G., Jr. (1994) Purification and properties of the *Escherichia coli* K-12 NAD-dependent nucleotide diphosphosugar epimerase, ADP-L-*glycero*-D-*manno*-heptose 6-epimerase, *J. Biol. Chem. 269*, 24384−24390.
10. Deacon, A. M., Ni, Y. S., Coleman, W. G., and Ealick, S. E. (2000) The crystal structure of ADP-L-*glycero*-D-*manno*-heptose 6-epimerase: Catalysis with a twist, *Structure 8*, 453−462.
11. Ni, Y., McPhie, P., Deacon, A., Ealick, S., and Coleman, W. G., Jr. (2001) Evidence that $NADP^+$ is the physiological cofactor of ADP-L-*glycero*-D-*manno*-heptose 6-epimerase, *J. Biol. Chem. 276*, 27329−27334.
12. Read, J. A., Ahmed, R. A., Morrison, J. P., Coleman, W. G., Jr., and Tanner, M. E. (2004) The mechanism of the reaction catalyzed by ADP-β-L-*glycero*-D-*manno*-heptose 6-epimerase, *J. Am. Chem. Soc. 126*, 8878−8879.
13. Read, J. A., Ahmed, R. A., and Tanner, M. E. (2005) Efficient chemoenzymatic synthesis of ADP-D-*glycero*-β-D-*manno*-heptose and a mechanistic study of ADP-L-*glycero*-D-*manno*-heptose 6-epimerase, *Org. Lett. 7*, 2457−2460.
14. Morrison, J. P., Read, J. A., Coleman, W. G., Jr., and Tanner, M. E. (2005) Dismutase activity of ADP-L-*glycero*-D-*manno*-heptose 6-epimerase: Evidence for a direct oxidation/reduction mechanism, *Biochemistry 44*, 5907−5915.
15. Meldal, M., Christensen, M. K., and Bock, K. (1992) Large-scale synthesis of D-mannose 6-phosphate and other hexose 6-phosphates, *Carbohydr. Res. 235*, 115−127.
16. García-Alles, L. F., Zahn, A., and Erni, B. (2002) Sugar recognition by the glucose and mannose permeases of *Escherichia coli*. Steady-state kinetics and inhibition studies, *Biochemistry 41*, 10077−10086.
17. Schoevaart, R., and Kieboom, T. (2001) Galactose dialdehyde: The forgotten candidate for a protein cross-linker? *Carbohydr. Res. 334*, 1−6.
18. Meynial, I., Paquet, V., and Combes, D. (1995) Simultaneous separation of nucleotides and nucleotide sugars using an ion-pair reversed-phase HPLC: Application for assaying glycosyltransferase activity, *Anal. Chem. 67*, 1627−1631.
19. Zamyatina, A., Gronow, S., Oertelt, C., Puchberger, M., Brade, H., and Kosma, P. (2000) Efficient chemical synthesis of the two anomers of ADP-L-*glycero*- and D-*glycero*-D-*manno*-heptopyranose allows the determination of the substrate specificities of bacterial heptosyltransferases, *Angew. Chem., Int. Ed. 39*, 4150−4153.
20. Yu, H., Yu, H., Karpel, R., and Chen, X. (2004) Chemoenzymatic synthesis of CMP-sialic acid derivatives by a one-pot two-enzyme system: Comparison of substrate flexibility of three microbial CMP-sialic acid synthetases, *Bioorg. Med. Chem. 12*, 6427−6435.
21. Abeles, R. H., and Lee, H. A., Jr. (1960) The dismutation of formaldehyde by liver alcohol dehydrogenase, *J. Biol. Chem. 235*, 1499−1503.
22. Hinson, J. A., and Neal, R. A. (1975) An examination of octanol and octanal metabolism to octanoic acid by horse liver alcohol dehydrogenase, *Biochim. Biophys. Acta 384*, 1−11.
23. Moxon, L. N., Holmes, R. S., Parsons, P. A., Irving, M. G., and Doddrell, D. M. (1985) Purification and molecular properties of alcohol dehydrogenase from *Drosophila melanogaster*: Evidence from NMR and kinetic studies for function as an aldehdye dehydrogenase, *Comp. Biochem. Physiol. 80B*, 525−535.

24. Eisses, K. T. (1989) On the oxidation of aldehdyes by alcohol dehydrogenase of *Drosophila melanogaster*: Evidence for the gem-diol as the reacting substrate, *Bioorg. Chem. 17*, 268−274.
25. Hara, A., Yamamoto, H., Deyashiki, Y., Nakayama, T., Oritani, H., and Sawada, H. (1991) Aldehdye dismutation catalyzed by pulmonary carbonyl reductase: Kinetic studies of chloral hydrate metabolism to trichloroacetic acid and trichloroethanol, *Biochim. Biophys. Acta 1075*, 61−67.
26. Henehan, G. T. M., and Oppenheimer, N. J. (1993) Horse liver alcohol dehydrogenase-catalyzed oxidation of aldehydes: Dismutation precedes net production of reduced nicotinamide adenine dinucleotide, *Biochemistry 32*, 735−738.
27. Henehan, G. T. M., Chang, S. H., and Oppenheimer, N. J. (1995) Aldehyde dehydrogenase activity of *Drosophila melanogaster* alcohol dehydrogenase: Burst kinetics at high pH and aldehyde dismutase activity at physiological pH, *Biochemistry 34*, 12294−12301.
28. Joernvall, H., Persson, B., Krook, M., Atrian, S., Gonzalez-Duarte, R., Jeffery, J., and Ghosh, D. (1995) Short-chain dehydrogenases/reductases (SDR), *Biochemistry 34*, 6003−6013.
29. Oppermann, U., Filling, C., Hult, M., Shafqat, N., Wu, X., Lindh, M., Shafqat, J., Nordling, E., Kallberg, Y., Persson, B., and Jörnvall, H. (2003) Short-chain dehydrogenases/reductases (SDR): The 2002 update, *Chem.-Biol. Interact. 143*−*144*, 247−253.
30. Naismith, J. H. (2006) Inferring the chemical mechanism from structures of enzymes, *Chem. Soc. Rev. 35*, 763−770.
31. Liu, Y., Thoden, J. B., Kim, J., Berger, E., Gulick, A. M., Ruzicka, F. J., Holden, H. M., and Frey, P. A. (1997) Mechanistic roles of tyrosine 149 and serine 124 in UDP galactose 4-epimerase from *Escherichia coli*, *Biochemistry 36*, 10675−10684.
32. Berger, E., Arabshahi, A., Wei, Y., Schilling, J. F., and Frey, P. A. (2001) Acid-base catalysis by UDP-galactose 4-epimerase: Correlations of kinetically measured acid dissociation constants with thermodynamic values for tyrosine 149, *Biochemistry 40*, 6699−6705.
33. Snipes, C. E., Brillinger, G.-U., Sellers, L., Mascaro, L., and Floss, H. G. (1977) Stereochemistry of the dTDP-glucose oxidoreductase reaction, *J. Biol. Chem. 252*, 8113−8117.
34. Allard, S. T. M., Beis, K., Giraud, M.-F., Hegeman, A. D., Gross, J. W., Wilmouth, R. C., Whitfield, C., Graninger, M., Messner, P., Allen, A. G., Maskell, D. J., and Naismith, J. H. (2002) Toward a Structural Understanding of the Dehydratase Mechanism, *Structure 10*, 81−92.
35. Blankenfeldt, W., Kerr, I. D., Giraud, M.-F., McMiken, H. J., Leonard, G., Whitfield, C., Messner, P., Graninger, M., and Naismith, J. H. (2002) Variation on a theme of SDR: dTDP-6-deoxy-L-lyxo-4-hexulose reductase (RmlD) shows a new Mg^{2+}-dependent dimerization mode, *Structure 10*, 773−786.
36. Somers, W. S., Stahl, M. L., and Sullivan, F. X. (1998) GDP-fucose synthetase from *Escherichia coli*: Structure of a unique member of the short-chain dehydrogenase/reductase family that catalyzes two distinct reactions at the same active site, *Structure 6*, 1601−1612.
37. Menon, S., Stahl, M., Kumar, R., Xu, G. Y., and Sullivan, F. (1999) Stereochemical course and steady state mechanism of the reaction catalyzed by the GDP-fucose synthetase from *Escherichia coli*, *J. Biol. Chem. 274*, 26743−26750.
38. Major, L. L., Wolucka, B. A., and Naismith, J. H. (2005) Structure and function of GDP-mannose-3′,5′-epimerase: An enzyme which performs three chemical reactions at the same active site, *J. Am. Chem. Soc. 127*, 18309−18320.
39. Ishiyama, N., Creuzenet, C., Lam, J. S., and Berghuis, A. M. (2004) Crystal structure of WbpP, a genuine UDP-N-acetylglucosamine 4-epimerase from *Pseudomonas aeruginosa*: Substrate specificity in UDP-hexose 4-epimerases, *J. Biol. Chem. 279*, 22635−22642.
40. Frey, P. A. (1996) The Leloir pathway, *FASEB J. 10*, 461−470.
41. Thoden, J. B., and Holden, H. M. (1998) Dramatic differences in the binding of UDP-galactose and UDP-glucose to UDP-galactose 4-epimerase from *Escherichia coli*, *Biochemistry 37*, 11469−11477.
42. Hallis, T. M., Zhao, Z., and Liu, H.-W. (2000) New insights into the mechanism of CDP-tyvelose 2-epimerase: An enzyme catalyzing epimerization at an unactivated stereocenter, *J. Am. Chem. Soc. 122*, 10493−10503.
43. Koropatkin, N. M., Liu, H.-W., and Holden, H. M. (2003) High resolution X-ray structure of tyvelose epimerase from *Salmonella typhi*, *J. Biol. Chem. 278*, 20847−20881.

BI602641M